Ab Initio Study of the Electronic Structure of XSO and XSO_2 (X = F, Cl) Radicals

Zhuangjie Li

The Department of Atmospheric Sciences, University of Illinois at Urbana−Champaign, Urbana, Illinois 61801

Received: August 4, 1997; In Final Form: September 22, 1997[⊗]

The geometry and vibrational frequency of XSO and XSO_2 (X = F, Cl) radicals in both the ground state and the first excited electronic state, as well as the transition energy between the two states have been studied using the ab initio method embodying Møller−Plesset perturbation theory with correlation energy correction truncated at the second-order (MP2) and fourth-order (MP4), and quadratic configuration interaction, including single and double substitution (QCISD). Both 6-31G* and 6-311G(2d) basis sets are used in the geometry optimization and frequency calculation, and the 6-311G(2df,2pd) basis set in the MP4 and QCISD single-point calculation. The same method is also applied to HSO, producing results in very good agreement with experiments. Molecular orbital calculations suggest that the $\tilde{A}^2A' \leftarrow \tilde{X}^2A''$ transition of the XSO radicals involves alternation from the σ^* antibonding orbital into the π^* antibonding orbital, and the $\tilde{A}^2A'' \leftarrow \tilde{X}^2A'$ transition of the XSO_2 radicals experiences the alternation of a nonbonding mixture of p_x, p_y, and p_z orbitals on the oxygen atoms into a bonding character. The vibrational frequency for S−O stretching of XSO and S−O asymmetric stretching of XSO_2 radicals is predicted to be lower in the excited state than in the ground state. The transition energies are best estimated to be 69.0, 55.8, 24.0, and 29.1 kcal mol^{-1} at QCISD/6-311G(2df,2pd)//MP2/6-311G(2d) + ΔZPE level of theory for FSO, ClSO, FSO_2, and $ClSO_2$, respectively, suggesting a low-lying excited electronic state for both FSO and FSO_2 radicals.

I. Introduction

Both XSO and XSO_2 (X = F, Cl) radicals are interesting species to study because of their roles in thionyl and sulfuryl halides chemistry.[1−7] FSO and ClSO have been found to be the major products for the photolysis of F_2SO and Cl_2SO at 193 and 248 nm, respectively.[2−5] FSO_2 can be produced in high temperature thermal decomposition of F_2SO_2.[6] The properties of these radicals and subsequent chemistry involving these radicals remain to be understood. From the standpoint of atmospheric chemistry, the interaction between atmospheric sulfur- and halogen-containing species is expected to increase due to the rising anthropogenic injection of hydrofluorocarbons (HFCs) such as HFC-125 (CF_3CHF_2) and HFC 134a (CF_3-CH_2F), which are used as chlorofluorocarbons (CFCs) substitutes as a result of implementation of the Montreal Protocol and its amendments. It has been postulated that FSO_2 can be generated as an intermediate species from the reaction of either FO_2 or CF_3O with SO_2:[7]

$$FO_2 + SO_2 \rightarrow FSO_2 + O_2 \quad (1)$$

$$CF_3O + SO_2 \rightarrow FSO_2 + CF_2O \quad (2)$$

and that FSO formed from further reaction of FSO_2 with O:

$$FSO_2 + O \rightarrow FSO + O_2 \quad (3)$$

Although both FSO and FSO_2 are likely to be produced in the atmosphere, there have been no atmospheric measurements made for these radicals so far. This may be due to very low atmospheric abundance of FSO and FSO_2, which depends on the competition between the formation rate of these radicals and their removal rate through either photolysis or reacting with other atmospheric species under atmospheric conditions. Moreover, the lack of characterization of FSO and FSO_2 radicals may be another factor limiting the atmospheric detection of these species since there is only finite information available for these radicals. FSO and ClSO were first separately observed by microwave spectroscopy and electron spin resonance (ESR) spectroscopy.[8,9] Both FSO and ClSO radicals were later detected by far-infrared laser magnetic resonance technique.[10] FSO_2 was identified only in a potassium sulfate matrix at 4 K by Sekhar et al.[11] Theoretically ab initio method was employed to study only the ground-state structure of FSO_2 and $ClSO_2$, and the first excited electronic structure of FSO at low levels of theory with small basis set.[12,13] The isomerization of FSO into FOS was recently studied by Muñoz et al.[14] More recently we reported the dissociation pathway study on XSO_2 radicals.[7] To further characterize both XSO and XSO_2 radicals we performed an ab initio study on the electronic structures for both XSO and XSO_2 radicals and report our results in this paper.

II. Computational Methods

Ab initio molecular orbital calculations were carried out using the GAUSSIAN 94 program.[15] The equilibrium geometry for both ground state and the first electronically excited state of XSO and XSO_2 radicals was fully optimized with analytical gradient at both Møller−Plesset correlation energy correction truncated at second-order (MP2) levels, and at Quadratic Configuration Interaction, including single and double substitutions (QCISD) level. Both 6-31G* and 6-311G(2d) basis sets were used in the optimization at MP2 level and 6-31G* basis set at QCISD level. Single point electron correlation was carried out using 6-311G(2df,2pd) basis set at both QCISD and MP4 levels with spin projection including single, double, triple, and quadruple excitations (PUMP4SDTQ, frozen core). Cartesian force constants were calculated analytically at MP2/6-311G-(2d) level, and numerically at QCISD/6-31G* level for both states of the XSO and XSO_2 radicals, and the resulting vibrational frequencies were computed after completion of each MP2/6-311G(2d) and QCISD/6-31G* optimization by determining the second derivatives of the energy with respect to the Cartesian nuclear coordinate and then transforming to mass-weighted coordinates.

[⊗] Abstract published in *Advance ACS Abstracts,* November 15, 1997.

S1089-5639(97)02572-3 CCC: $14.00

III. Results and Discussion

A. Electronic States of the XSO and XSO_2 Radicals. It is known that the ground-state XSO and XSO_2 radicals belong to the C_s symmetry group,[7,12,13] indicating a nonlinear structure for FSO and ClSO and a nonplanar structure for FSO_2 and $ClSO_2$ species, respectively. There are 7 and 9 molecular orbitals (MOs) with a″ symmetry in ground-state FSO and ClSO, respectively, resulting in a $\tilde{X}^2A''$ ground state for these two radicals. The first electronically excited state of both FSO and ClSO radicals has 8 and 10 a″ MOs which lead to an $\tilde{A}^2A'$ first excited state for the XSO radicals. The ground-state orbital symmetries of FSO_2 and $ClSO_2$ are predicted to possess 14 and 16 molecular orbitals with a″ symmetry, respectively, resulting in a ground state of $\tilde{X}^2A'$ for both radicals. In contrast, the first electronic excited state of both FSO_2 and $ClSO_2$ has one molecular orbital of a″ symmetry less than their corresponding ground state, giving rise to an $\tilde{A}^2A''$ state as the first excited state for the XSO_2 radicals. The unrestricted Hartree−Fock (UHF) calculation predicts an alpha MO for the highest occupied molecular orbital (HOMO) and a beta MO for the lowest unoccupied molecular orbital (LUMO) for the open shell XSO and XSO_2 species, and the occupation of the LUMO by an electron in the beta orbital leads to the first electronically excited state. The first excited electronic state of the ClSO, FSO_2, and $ClSO_2$ radicals was accordingly obtained by promoting an electron from the highest occupied beta orbital featuring an a′, a″, and a″ orbital symmetry, into the corresponding radical LUMO featuring an a″, a′, and a′ symmetry, respectively. In the case of FSO, since the highest occupied beta MO and the LUMO are both in a″ symmetry, promoting the electron from the HOMO into the LUMO will not lead to an $\tilde{A}^2A'$ state. The second highest occupied beta MO of the ground-state FSO has an a′ symmetry and the $\tilde{A}^2A'$ state of FSO is then obtained by promoting the electron occupying the second highest occupied beta MO into the LUMO.

The molecular orbitals characterizing both ground state and the first electronic excited states of XSO and XSO_2 radicals are shown in Figure 1. The LUMO of the radicals in ground states is related to the HOMO of the excited state of the radicals and vice versa. In fact, structural optimization following the HOMO/LUMO switching leads to the interchange between the ground state and the first excited state for these radicals. The HOMO of both ground state FSO and ClSO predicts that the MO consists mainly of s orbitals on sulfur atom, and p_x plus p_y orbitals on oxygen and halogen atoms, with a S−O and a X−S σ^* antibonding character. The LUMO of the XSO radicals consists mainly of p_z orbital on the sulfur, oxygen, and the halogen atoms, which shows a S−O and a X−S π^* antibonding feature. Since the occupation of the LUMO with an electron leads to the $\tilde{A}^2A'$ state in XSO radicals, the electronic transition of the XSO radicals is accordingly a $\sigma^* \leftrightarrow \pi^*$ type transition. Sakai and Morokuma[13] suggested a nonbonding n-type orbital (12a′) into the SO antibonding π^* (4a″) orbital in their ab initio study of the FSO radical going from ground state to the first excited electronic state, which defers our result of turning S−O antibonding σ^* (13a′) orbital into the S−O antibonding π^*-(4a″) orbital. We examined the 12a′ orbital and found that instead of a nonbonding n-type orbital on oxygen, the 12a′ MO includes an S−O σ bonding and an F−S π^* antibonding feature. As shown in Figure 1, the LUMO of FSO in $\tilde{A}^2A'$ state does not possess a feature of nonbonding orbital on oxygen atom, but carry a σ antibonding feature for F−S bond and a π bonding feature for S−O bond, suggesting that that orbital is not originated from a n-type orbital. Furthermore, the MOs involved in the $\tilde{A}^2A' \leftrightarrow \tilde{X}^2A''$ electronic transition for FSO are similar

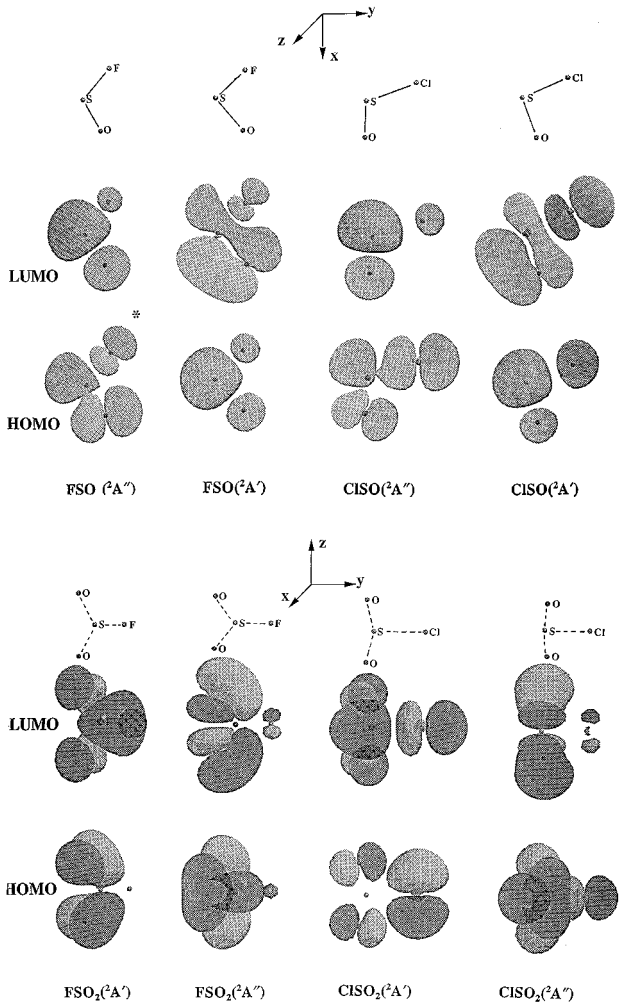

Figure 1. Highest occupied β molecular orbital (HOMO) and the lowest unoccupied molecular orbital (LUMO) of XSO and XSO_2. The MOs are calculated at MP2/6-311G(2d) level of theory. * indicates the second highest occupied β molecular orbital.

to that for ClSO since these two radicals share the same type of transition, and no n-type orbital on oxygen is found in the ClSO radical. Therefore, the $\tilde{A}^2A' \leftrightarrow \tilde{X}^2A''$ transition of the FSO radical should be a $\sigma^* \leftrightarrow \pi^*$ type transition other than a $n \leftrightarrow \pi^*$ type transition. The first electronic transition of FSO_2 involves changing of the nonbonding p_x, p_y and p_z orbitals on oxygen atoms into a bonding character, in which the P_x orbitals on two oxygen atoms overlap, causing a dramatic change in the molecular structure. For $ClSO_2$, the nonbonding p_z orbital on chlorine atom and p_y orbital on the oxygen atoms are changed into bonding orbitals mainly consisting of p_y orbital on both chlorine and sulfur atoms, and p_x, p_y, and p_z orbitals on oxygen atoms. Again the overlapping of the p_x orbitals on the oxygen atoms of the $ClSO_2$ radical gives rise to a large change on the radical structure going from the ground state to the first excited state.

B. Geometries. The calculated geometries along with the available experimental structure for the XSO and XSO_2 radicals in both the ground state and the first excited state are given in Table 1. The radical structures are optimized at MP2 level with both 6-31G* and 6-311G(2d) basis sets, and at QCISD level of theory with the 6-31G* basis set. To test the reliability of the computational methods, we performed optimization calculations for HSO radical, bearing some analogy to XSO, at the same levels of theory, and the results are presented in the Table 1. The calculated bond lengths and bond angles for HSO radical in both ground state ($\tilde{X}^2A''$) and the first excited state ($\tilde{A}^2A'$)

TABLE 1: Optimized Geometry for HSO, XSO, and XSO_2 (X = Cl, F) in $^2A'$ and $^2A''$ States[a]

		$^2A'$ state				$^2A''$ state			
		QCISD 6-31G*	MP2 6-31G*	MP2 6-311G(2d)	exptl[b]	QCISD 6-31G*	MP2 6-31G*	MP2 6-311G(2d)	exptl[b]
HSO	*r*(H−S)	1.352	1.344	1.356	1.34	1.371	1.368	1.388	1.35
	r(S−O)	1.707	1.700	1.687	1.69	1.545	1.492	1.475	1.54
	∠(H−S−O)	91.9	91.6	92.2	97	104.3	106.6	106.5	102
FSO	*r*(F−S)	1.636	1.631	1.621		1.639	1.641	1.636	1.602
	r(S−O)	1.721	1.713	1.707		1.483	1.459	1.449	1.452
	∠(F−S−O)	92.9	93.6	93.7		108.4	111.4	110.5	108.3
FSO_2	*r*(F−S)	1.619	1.627	1.613		1.622	1.624	1.614	
	r(S−O)	1.463	1.461	1.441		1.531	1.524	1.509	
	∠(F−S−O)	105.9	106.5	106.9		103.3	105.0	104.8	
	∠(O−S−O)	123.5	124.8	124.6		92.5	89.5	90.1	
	∠DIH	−132.7	−135.1	−135.5		−95.9	−93.6	−94.1	
ClSO	*r*(Cl−S)	2.044	2.027	2.048		2.088	2.092	2.119	
	r(S−O)	1.709	1.705	1.693		1.499	1.457	1.449	
	∠(Cl−S−O)	92.8	93.4	93.1		109.3	112.6	112.1	
$ClSO_2$	*r*(Cl−S)	2.149	2.121	2.129		2.094	2.089	2.116	
	r(S−O)	1.465	1.465	1.446		1.542	1.533	1.514	
	∠(Cl−S−O)	107.8	108.1	108.3		105.0	106.4	106.0	
	∠(O−S−O)	122.4	123.7	123.7		92.2	89.2	89.9	
	∠DIH	−134.0	−136.2	−136.4		−96.5	−94.1	−94.7	

[a] Bond lengths are in Å and bond angles are in degree. [b] Data are from refs 8 and 17.

are in very good agreement with the experimental observations, with differences of less than 0.04 Å in the bond lengths and 6° in the bond angles at all levels of theory employed. Similar accuracy is also observed for the FSO ground-state structure prediction using the same methods, in which the calculated ∠(F−S−O) bond angle differs from the experimental value by ca. 3°. The good agreement between the calculation and experimental measurements suggests that the XSO and XSO_2 radical structure may be predicted with an uncertainty of less than 5% at the MP2/6-31G*, MP2/6-311G(2d), and QCISD/6-31G* levels of theory.

Like the ground state, the molecular structure of both XSO and XSO_2 radicals in the first excited electronic state is found to possess C_s symmetry. Using the 6-31G* basis set, there is little difference between MP2 and QCISD methods in predicting the structure for both states of the XSO and XSO_2 radicals. The optimized FSO ground-state structure using the 6−311(2d) basis set agrees better with the experiment than using the 6-31G* basis set, probably due to the increase flexibility of the triple valance zeta basis.

While there is little changes in the X−S bond length, a large S−O bond length change is predicted for the XSO radicals going from the ground state to the first excited state, and at MP2/6-311G(2d) level of theory the S−O bond increases from 1.449 to 1.707 Å for FSO and to 1.693 Å for ClSO radicals, respectively. There is also about an 18° decrease in the ∠(X−S−O) angles associated with the $\tilde{A}^2A' \leftarrow \tilde{X}^2A''$ electronic transition of the XSO radicals. The increase of the S−O bond length and decrease of the ∠(X−S−O) angles result from the change of the β occupied molecular orbitals from a σ^* character to a π^* character, in which the repulsion of the antibonding p_z orbitals between sulfur and oxygen atoms pushes the oxygen and sulfur atoms further away from each other, and the attraction of the p_z orbitals between halogen and oxygen atoms tends to pull these two atoms close to each other.

The X−S bonds in the XSO_2 remain basically unchanged since 1.613 Å, 1.614 Å, and 2.048 Å, 2.119 Å are predicted at MP2/6-311G(2d) level for FSO_2 and $ClSO_2$ in the ground state and the first excited state, respectively. The S−O bond is slightly increased, however, from 1.441 Å to 1.509 Å for FSO_2, and from 1.446 Å to 1.514 Å for $ClSO_2$, respectively. The ∠(X−S−O) angles are found to slightly decrease, but the ∠(O−S−O) angles are predicted to be substantially reduced from 124.6° to 90.1° for FSO_2, and from 123.7° to 89.9° for $ClSO_2$ for the $\tilde{A}^2A'' \leftarrow \tilde{X}^2A'$ transition, respectively. The decrease of the ∠(O−S−O) angles by ca. 30° in the electronic transition of the XSO_2 radicals arises from the overlapping of the p_x and p_z components of the atomic ortibals on two oxygen of the XSO_2 radicals. These atomic orbital interactions also cause the XSO_2 radicals to become more nonplanar after being electronically excited, as indicated by 40° decrease in dihedral angles of the radicals.

C. Frequencies. The vibrational frequencies for the XSO and XSO_2 radicals in both ground state and the first excited state at both MP2 and QCISD levels of theory, and the results are given in Table 2. It is known that the frequency obtained at MP2/6-31G* level for ground-state FSO overestimates the S−O stretching by ∼30%.[7] The use of larger basis set slightly improves the S−O stretching frequency, but the agreement with the experiment is still far from satisfactory. For the XSO_2 radicals, the MP2 frequency calculations produce the S−O asymmetric stretching of 2350 and 2043 cm^{-1} for the FSO_2 and $ClSO_2$ radicals, respectively. This suggests a serious accuracy problem for vibrational frequency evaluation of XSO_2 radicals at the MP2 level, since the S−O asymmetric stretching frequency in the excited state should be lower than that of the ground state due to the longer S−O bonds. To better quantify the vibrational frequencies for the XSO and XSO_2 radicals we again use HSO as a test case for the appropriateness of other methods, and we found very good agreement in vibrational frequencies between that calculated at QCISD/6-31G* level of theory and that measured experimentally for both ground state and the first excited state of the HSO radical, with a difference of less than 80 cm^{-1} for H−S stretching, S−O stretching, and H−S−O bending motions. Another test for the accuracy of the QCISD/6-31G* frequency calculation is the application of this method to the FSO radical. It can be seen from Table 2 that the FSO ground-state frequencies obtained at the QCISD/6-31G* level differ from the experimental value by less than 50 cm^{-1}, showing a significant improvement in agreement with the experiment compared to the MP2/6-311G(2d) level of theory. This indicates a better method of using QCISD/6-31G* than using MP2/6-311G(2d) for evaluating vibrational frequencies for both XSO and XSO_2 radicals.

Listed in Table 2 are also the vibrational mode assignment for each frequency of the XSO and XSO_2 radicals in both ground and the first excited electronic states. For the FSO_2 and $ClSO_2$ radicals, some low frequency vibrations involve coupling of

TABLE 2: Frequencies (in cm^{-1}) for HSO, XSO, and XSO_2 (X = Cl, F) Radicals[a]

species	$\langle S^2 \rangle$	elec state	mode	symm	description	frequency	IR int	exptl[b]
HSO	0.778	$\tilde{X}^2A''$	1	a′	H−S stretching	2500	1.0	2570
			2	a′	S−O stretching	941		1013
			3	a′	H−S−O bending	1085		1063
	0.763	$\tilde{A}^2A'$	1	a′	H−S stretching	2675	0.23	2769
			2	a′	H−S−O bending	878	1.00	828
			3	a′	S−O stretching	724		702
FSO	0.779	$\tilde{X}^2A''$	1	a′	S−O stretching	1165	0.22	1215
			2	a′	F−S stretching	798	1.00	763
			3	a′	F−S−O bending	379	0.10	396
	0.762	$\tilde{A}^2A'$	1	a′	S−O stretching	736	0.34	
			2	a′	F−S stretching	828	1.00	
			3	a′	F−S−O bending	279	0.14	
FSO_2	0.779	$\tilde{X}^2A'$	1	a″	S−O asym str	1253	0.41	
			2	a′	S−O sym str	1088	0.36	
			3	a′	F−S stretching	793	1.00	
			4	a′	FSO_2 umbrella	509	0.14	
			5	a′	FSO_2 rocking	406	0.11	
			6	a″	FSO_2 wagging	382	0.12	
	0.812	$\tilde{A}^2A''$	1	a″	S−O asym str	809	1.00	
			2	a′	S−O sym str	1081	0.50	
			3	a′	F−S stretching	820	0.10	
			4	a′	FSO_2 umbrella	497	0.20	
			5	a′	FSO_2 rocking	379		
			6	a″	FSO_2 wagging	296		
ClSO	0.780	$\tilde{X}^2A''$	1	a′	S−O stretching	1099	0.48	
			2	a′	Cl−S stretching	477	1.00	
			3	a′	Cl−S−O bending	294		
	0.778	$\tilde{A}^2A'$	1	a′	S−O stretching	719	0.49	
			2	a′	Cl−S stretching	512	1.00	
			3	a′	Cl−S−O bending	218	0.27	
$ClSO_2$	0.803	$\tilde{X}^2A'$	1	a″	S−O asym str	1299	1.00	
			2	a′	S−O sym str	1081	0.74	
			3	a′	Cl−S stretching	489	0.71	
			4	a′	$ClSO_2$ umbrella	420	0.69	
			5	a′	$ClSO_2$ rocking	247		
			6	a″	$ClSO_2$ wagging	214	0.11	
	0.813	$\tilde{A}^2A''$	1	a″	S−O asym str	784		
			2	a′	S−O sym str	1030	0.68	
			3	a′	Cl−S stretching	501	1.00	
			4	a′	O−S−O bending	430	0.19	
			5	a′	$ClSO_2$ rocking	298		
			6	a″	$ClSO_2$ wagging	217		

[a] Frequencies are computed at QCISD/6-31G* level with geometry optimized at the same level. IR intensities are relative to the strongest band of the species. [b] Data are from refs 33−35.

more than one motion, and the vibrational mode assignments become difficult. Under such cases only the dominant vibrational motion is presented.

At the QCISD/6-31G* level of theory, the S−O stretching frequencies of the XSO radicals are predicted to be 1165 cm^{-1} in the ground state and 736 cm^{-1} in the first excited state for FSO, and 1099 cm^{-1} in the ground state and 719 cm^{-1} in the first excited state for ClSO, respectively. The low S−O stretching frequency in the excited state of the XSO radicals correspond to a substantial S−O bond increase due to the excitation. Similar trends are also predicted for the S−O asymmetric stretching frequency of both FSO_2 and $ClSO_2$ radicals, which are 1253 cm^{-1} in the ground state and 809 cm^{-1} in the first excited state for FSO_2, and 1299 cm^{-1} in the ground state and 784 cm^{-1} in the first excited state for $ClSO_2$, respectively. The other vibrational frequencies of the XSO and XSO_2 radicals are not significantly altered during the electronic transition. Note that the X−S stretching frequency of XSO decreases when the hydrogen atom of the HSO is substituted by a fluorine atom, and further decreases when substituted by a chlorine atom, which is expected due to the increase of the reduced mass of the radical after the substitution. Finally, the frequency calculation at QCISD/6-31G* level of theory assigns the most intense infrared peak to the X−S stretching for both XSO and XSO_2 radicals in ground state, except $ClSO_2$, in which the S−O asymmetric stretching mode has maximum intensity for the infrared absorption.

D. Transition Energy. The adiabatic transition energy is evaluated for both XSO and XSO_2 radicals by calculating the total energy difference between the ground state and the first excited state of the radicals optimized at QCISD/6-31G*, MP2/6-31G*, and MP2/6-311G(2d) levels of theory. All single point energy computations are performed using the 6-311G(2df,2pd) basis set and the radical geometries in both states optimized at MP2/6-311G(2d) level. The transition energy is further corrected by adding the radical zero point energy difference between the ground state and the first excited state using the calculated vibrational frequencies from Table 2. Table 3 presents the calculated transition energy along with the calculated total energy for both XSO and XSO_2 radicals in both the lower and the upper states. Since there is no experimental data available for the electronic transition of these radicals, the first electronic transition energy for HSO is calculated to assess the accuracy of the levels of theory applied to the XSO and XSO_2 radicals, and the results are also presented in the Table 3. Comparison of the results at the MP2/6-31G* and MP2/6-311G(2d) levels shows that the large basis set significantly improves the agreement with the experimental measurement for the first electronic transition of HSO. Higher order perturbation corrections decreases the transition energy by 2 kcal mol^{-1}, and

TABLE 3: Calculated Energies

Calculated Energy (in kcal mol^{-1}) for the First Electronic Transition of HSO, XSO, and XSO_2 (X = Cl, F) Radicals

	HSO ($\tilde{A}^2A' \leftarrow \tilde{X}^2A''$)	FSO ($\tilde{A}^2A' \leftarrow \tilde{X}^2A''$)	FSO_2 ($\tilde{A}^2A'' \leftarrow \tilde{X}^2A'$)	ClSO ($\tilde{A}^2A' \leftarrow \tilde{X}^2A''$)	$ClSO_2$ ($\tilde{A}^2A'' \leftarrow \tilde{X}^2A'$)
QCISD/6-31G*	33.8	62.8	16.9	50.8	22.9
MP2/6-31G*	35.8	71.6	26.4	57.8	32.5
MP2/6-311G(2d)	41.8	78.6	31.5	65.8	36.6
MP4SDTQ/6-311G(2df,2pd)[a]	39.8	74.8	26.1	61.5	31.7
PMP4SDTQ/6-311G(2df,2pd)[a]	40.1	75.2	24.5	61.7	30.9
QCISD/6-311G(2df,2pd)[a]	37.5	69.8	23.2	56.3	28.4
Δzero point energy[a]	−0.4	−0.8	0.8	−0.5	0.7
QCISD/6-311G(2df,2pd) + ΔZPE	37.1	69.0	24.0	55.8	29.1
exptl[b]	41.0				

Calculated Total Energy (in Hartree) for HSO, XSO and XSO_2 (X = Cl, F) Radicals

	QCISD/ 6-31G*	MP2/ 6-31G*	MP2/ 6-311G(2d)	MP4SDTQ[c]/ 6-311G(2df,2pd)	PMP4SDTQ[c]/ 6-311G(2df,2pd)	QCISD[c]/ 6-311G(2df,2pd)
HSO(^{2}A″)	−473.199 82	−473.170 71	−473.279 70	−473.383 78	−473.386 09	−473.369 00
HSO(^{2}A′)	−473.146 00	−473.113 72	−473.213 10	−473.320 35	−473.322 15	−473.309 30
FSO(^{2}A″)	−572.234 47	−572.219 32	−572.412 29	−572.529 87	−572.532 26	−572.500 78
FSO(^{2}A′)	−572.134 44	−572.105 25	−572.287 11	−572.410 72	−572.412 47	−572.389 56
FSO_2(^{2}A′)	−647.227 96	−647.222 58	−647.480 85	−647.632 20	−647.634 49	−647.587 37
FSO_2(^{2}A″)	−647.201 05	−647.180 48	−647.430 73	−647.590 63	−647.595 52	−647.550 42
ClSO(^{2}A″)	−932.248 70	−932.219 48	−932.389 70	−932.528 84	−932.531 28	−932.499 14
ClSO(^{2}A′)	−932.167 70	−932.127 35	−932.284 85	−932.430 79	−932.432 95	−932.409 41
$ClSO_2$(^{2}A′)	−1007.239 65	-−1007.223 35	−1007.458 19	−1007.630 60	−1007.634 32	−1007.582 91
$ClSO_2$(^{2}A″)	−1007.203 18	-−1007.171 51	−1007.399 90	−1007.580 08	−1007.585 09	−1007.537 60

[a] Using frequencies calculated at QCISD/6-31G* level of theory with geometry optimized at the same level for both ^{2}A′ and ^{2}A″ states. [b] From ref 17. [c] Single-point calculation using the radical geometry optimized at the MP2/6-311G(2d) level of theory.

the spin projection has little effect on the transition energy due to the low spin contamination of the radical (see $\langle S^2 \rangle$ of Table 2). A value of 40.1 kcal mol^{-1} for the first electronic transition energy is obtained from the PMP4SDTQ/6-311G(2df,2pd)// MP2/6-311G(2d) single point calculation, which agrees very well with the experimental value of 41.0 kcal mol^{-1}. The single point calculation at QCISD/6-311G(2df,2pd)//MP2/6-311G(2d) level is lowered by 2.6 kcal mol^{-1} compared to that at the PMP4SDTQ/6-311G(2df,2pd)//MP2/6-311G(2d) level. Similar basis set and spin projection effects are observed in evaluating the first electronic transition for both XSO and XSO_2 radicals, and the transition energy is predicted to be 75.2 kcal mol^{-1}, 61.7 kcal mol^{-1}, 24.5 kcal mol^{-1} and 30.9 kcal mol^{-1} at the PMP4SDTQ single point level and 69.8 kcal mol^{-1}, 56.3 kcal mol^{-1}, 23.2 kcal mol^{-1}, and 28.4 kcal mol^{-1} at the QCISD single point level for FSO, ClSO, FSO_2, and $ClSO_2$, respectively. Although the QCISD single point calculation slightly underestimates the transition energy for HSO, it is chosen for the best estimated energetics for HSO, XSO and XSO_2 electronic transitions since this method takes into account to some extent the configuration interactions by including single and double substitutions of the Hartree−Fock single-determinant in the truncated configuration space of the substitutions. Thus with the consideration of zero point energy correction, the best estimated value for the first electronic transition of the XSO and XSO_2 radicals is determined by QCISD/6-311G(2df,2pd) + ΔZPE, which becomes 69.0, 55.8, 24.0, and 29.1 kcal mol^{-1} for FSO, ClSO, FSO_2, and $ClSO_2$, respectively. While there are very little experimental data available for the electronic transition of the XSO and XSO_2 radicals, it is conceivable that the transition energy estimation for these radicals would carry an uncertainty similar to that of HSO, which is about 4 kcal mol^{-1}.

The reaction enthalpy for halogen atom extrusion from the XSO and XSO_2 radicals has been estimated to be ca. 79 kcal mol^{-1} and 46 kcal mol^{-1} for FSO and ClSO, and 28.7 kcal mol^{-1} and −7.7 kcal mol^{-1} for FSO_2 and $ClSO_2$, respectively.[7,16] The transition energy for FSO and FSO_2 is then ca. 10 kcal mol^{-1} and 4.7 kcal mol^{-1} lower than the dissociation enthalpy, suggesting that the first excited electronic state of both FSO and FSO_2 radicals is a low lying excited electronic state.

The results from the present study suggest that the first electronic transition occurs at 24,150 cm^{-1}, 19,530 cm^{-1}, 8,400 cm^{-1}, and 10,180 cm^{-1} for the FSO, ClSO, FSO_2, and $ClSO_2$ radicals. In studying the photofragmentation of thionyl chloride, Baum et al.[4] suggested that ClSO has an excited electronic state at ca. 9,000 cm^{-1}, based on their analysis of the fragment kinetic distribution of the radical channel due to the photolysis of Cl_2SO at 248 and 193 nm. They proposed that the 26 kcal mol^{-1} of energy arising from the difference between the maximum translational energy of ClSO and the energy available after the rupture of a Cl−S bond in Cl_2SO photolysis will be used to excite the ClSO radical to the first excited electronic state. Present calculation on the ClSO electronic transition energy indicates that the 26 kcal mol^{-1} energy is insufficient in populating such an excited electronic state. It is likely, however, that this excess amount of energy may be used to excite the ClSO radical to the vibrationally excited states in the ground state.

IV. Summary

We have investigated the ground state and the first excited electronic state of both XSO and XSO_2 radicals using ab initio method. The radical structures are calculated at MP2/6-31G*, MP2/6-311G(2d), and QCISD/6-31G* levels of theory, and the frequencies are evaluated at both MP2/6311G(2d) and QCISD/6-31G* levels. The transition energy between the two states of the XSO and XSO_2 radicals are estimated by performing single point calculation at MP4 and QCISD level with 6-311G-(2df.2pd) basis set. These methods are applied to HSO radical for accuracy checking, and they produce results in very good agreement with experiments. The $\tilde{A}^2A' \leftarrow \tilde{X}^2A''$ transition of the XSO radicals involves changing σ^* antibonding orbitals into π^* antibonding orbitals, and the $\tilde{A}^2A'' \leftarrow X^2A'$ transition of the XSO_2 radicals experiences the alternation of nonbonding

mixture of p_x, p_y, and p_z orbitals on the oxygen atoms into a bonding character. As a result of the molecular orbital changes due to the electronic transition, the S−O bond increases by ca. 0.25 Å in FSO and ClSO, and by ca. 0.07 Å in FSO_2 and $ClSO_2$, and the bond angles, ∠(X−S−O) in the XSO, and ∠(O−S−O) in the XSO_2 radicals decrease by more than 15° and 30°, respectively. The S−O stretching vibration in the XSO radicals and the asymmetric S−O stretching vibration in the XSO_2 radicals are predicted to be substantially lower in the first excited state than in the ground state. Finally, the transition energies are estimated to be 69.0 kcal mol^{-1}, 55.8 kcal mol^{-1}, 24.0 kcal mol^{-1}, and 29.1 kcal mol^{-1} for FSO, ClSO, FSO_2, and $ClSO_2$, respectively, suggesting a low lying excited electronic state for both FSO and FSO_2 radicals.

Acknowledgment. The author thanks NCSA for supercomputer time support to this work and Professor J. S. Francisco for helpful discussions.

References and Notes

(1) Patai, S.; Rapporport, Z.; Stirling, C., Eds., The chemistry of sulphones and sulphoxides Wiley: New York, 1988, p 33.
(2) Wang. H.; Chen, X.; Weiner, B. R. *Chem. Phys. Lett.* **1993**, *216*, 537.
(3) Wang. H.; Chen, X.; Weiner, B. R. *J. Phys. Chem.* **1993**, *97*, 12260.
(4) Baum, G.; Effenhauser, C. S.; Felder, P.; Huber, J. R. *J. Phys. Chem.* **1992**, *96*, 756.
(5) Kawasaki, M.; Kasatani, K.; Sato, H. *Chem. Phys.* **1984**, *91*, 285.
(6) Wray, K. L.; Feldman, E. V. *J. Chem. Phys.* **1971**, *54*, 3445.
(7) Li, Z. *Chem. Phys. Lett.* **1997**, *269*, 128.
(8) Endo, Y.; Saito, S.; Hirota, E. *J. Chem. Phys.* **1981**, *74*, 1568.
(9) Nishikida, K.; Williams, F. *J. Magn. Reson.* **1974**, *14*, 348.
(10) Radford, H. *J. Mol. Spectrosc.* **1983**, 99, 209.
(11) Sekhar, Y. R.; Bill, H.; Lovy, D. *Chem. Phys. Lett.* **1987**, *136*, 57.
(12) Boyd, R. J.; Gupta, A.; Langler, R. F.; Lownie, S. P.; Pincock, J. A. *Can. J. Chem.* **1980**, *58*, 331.
(13) Sakai, S.; Morokuma, K. *Chem. Phys.* **1980**, 52, 33.
(14) Muñoz, L. A.; Weiner, B. R.; Ishikawa, Y. *J. Mol. Struct.: THEOCHEM* **1996**, *388*, 1.
(15) Frisch, M. J.; Trucks, G. W.; Schlegel, H. B.; Gill, P. M. W.; Johnson, B. G.; Robb, M. A.; Cheeseman, J. R.; Keith, T.; Petersson, G. A.; Montgomery, J. A.; Raghavachari, K.; Al-Laham, M. A.; Zakrzewski, V. G.; Ortiz, J. V.; Foresman, J. B.; Peng, C. Y.; Ayala, P. Y.; Chen, W.; Wong, M. W.; Andres, J. L.; Replogle, E. S.; Gomperts, R.; Martin, R. L.; Fox, D. J.; Binkley, J. S.; Defrees, D. J.; Baker, J.; Stewart, J. P.; Head-Gordon, M.; Gonzalez, C.; Pople, J. A. *GAUSSIAN 94*; Gaussian, Inc.: Pittsburgh, 1995.
(16) Tao, Z.; Li, Z. *Chem. Phys. Letts.*, in preparation.
(17) Schurath, U.; Weber, M.; Becker, K. H. *J. Chem. Phys.* **1977**, *67*, 110.